Protoplasma (2000) 212: 46–55

PROTOPLASMA

Atomic-force microscopy imaging of plasma membranes purified from spinach leaves

M. Crèvecoeur[1,*], **E. Lesniewska**[2], **V. Vié**[2], **J. P. Goudonnet**[2], **H. Greppin**[1], and **C. Le Grimellec**[3]

[1] Physiologie et Biochimie Végétales, Université de Genève, Geneva, [2] Laboratoire de Physique, CNRS 5027, Université de Bourgogne, Dijon, and [3] Centre de Biochimie Structurale, INSERM U414, Université de Montpellier, Montpellier

Received August 18, 1999
Accepted December 6, 1999

Summary. Plasma membranes purified from spinach leaves by aqueous two-phase partitioning were examined by atomic-force microscopy (AFM) in phosphate buffer, and details on their structure were reported at nanometric scale. Examination of the fresh membrane preparation deposited on mica revealed a complex organization of the surface. It appeared composed of a first layer of material, about 8 nm in thickness, that practically covered all the mica surface and on which stand structures highly heterogeneous in shape and size. High-resolution imaging showed that the surface of the first layer appeared relatively smooth in some regions, whereas different characteristic features were observed in other regions. They consisted of globular-to-elliptical protruding particles of various sizes, from 4–5 nm x-y size for the smallest to 40–70 nm for the largest, and of channel-like structures 25–30 nm in diameter with a central hole. Macromolecular assemblies of protruding particles of various shapes were imaged. Addition of the proteolytic enzyme pronase led to a net roughness decrease in regions covered with particles, indicating their proteinaceous nature. The results open fascinating perspectives in the investigation of membrane surfaces in plant cells with the possibility to get structural information at the nanometric range.

Keywords: Atomic-force microscopy; Plasmalemma; Phase partition; Leaf cells; Spinach.

Abbreviations: AFM atomic-force microscopy; EM electron microscopy; TMAFM tapping-mode atomic-force microscopy.

Introduction

In plants the plasma membrane, the outer permeability barrier of the cell, has a number of essential physiological functions. These include transport of ions and other solutes out and into the cells, hormone binding and response, synthesis and assembly of cell wall materials. The plasma membrane plays an important role in interactions with pathogens and in perception of external environmental signals with their subsequent transmission into the cells, where a cascade of events is triggered (Leshem 1992, Lebrun-Garcia et al. 1999). A key role has also been proposed for this membrane in some growth and development processes (Greppin et al. 1991, Leshem 1992, Masson et al. 1994). Knowledge of the structural organization of the plasma membrane is a fundamental recognized step in understanding its different cellular functions in relation with such processes. Part of this knowledge has been acquired by current electron microscopy (EM) which, unfortunately, does not allow the observation of native membranes. Biophysical methods have proved to be also useful for a clearer understanding of organization and dynamics of the plasma membrane (Quinn and Williams 1990, Leshem 1992).

The atomic-force microscope (AFM), invented by Binnig et al. (1986), allows the surface of biological samples to be imaged at high resolution under physiological conditions and has been used to image a wide variety of biological samples, among them have been membranes, both native and reconstituted. It is actually considered as a powerful tool for the study of membrane surfaces with reproducibility and with a lateral resolution of about 0.5 nm and an extraordinary vertical resolution of about 0.1 nm (Danker et al. 1997, Lesniewska et al. 1998, Müller et al. 1999). This is much higher than that of light microscopes and comparable with electron microscopes, with the great

* Correspondence and reprints: Physiologie et Biochimie Végétales, Université de Genève, 3 Place de l'Université, CH-1211 Genève 4, Switzerland.

advantage to observe samples in buffer without particular preparation (Lal and John 1994, Shao et al. 1996). Membrane surfaces of different intact cells have been directly examined by AFM in buffer or in their growth medium (Butt et al. 1990a, 1991; Henderson et al. 1992; Häberle et al. 1991; Hörber et al. 1992; Le Grimellec et al. 1994; Oberleithner et al. 1997). The AFM has been used to image the surface topography of natural and reconstituted two-dimensional crystals of membrane proteins such as gap junctions, bacteriorhodopsin, cholera toxin, and *Escherichia coli* porin in aqueous conditions without fixation (Butt et al. 1990b, 1991; Hoh et al. 1991, 1993; Schabert et al. 1995; Heymann et al. 1997). Images of isolated biological membranes have been reported for plasma membrane (Le Grimellec et al. 1995, Lärmer et al. 1997) and nuclear envelope (Danker et al. 1997, Rakowska et al. 1998). So far, however, in spite of the great qualities and potentialities offered by AFM to investigate native membrane surfaces, it does not appear to have been used for high-resolution imaging of the plasma membrane in plant cells. In plants, this membrane is accessible with difficulty due to the presence of the cell wall. Part of our knowledge of fine structure of this membrane comes from studies with protoplasts that are routinely obtained from a great variety of plant tissues (Fowke 1986, 1988; Fowke et al. 1986; Leshem 1992). Another approach consists in preparing a highly purified fraction of this membrane, with partition in aqueous dextran-polyethylene glycol (PEG) two-phase systems as the most common method used. This procedure separates the membrane vesicles according to their surface properties. The plasma membrane-derived vesicles are preferentially found in the PEG-rich upper phase and are essentially cytoplasmic side-in (Körner et al. 1985, Larsson et al. 1987, Sandstrom et al. 1987, Sandelius and Morré 1990). Two-phase partitioning is routinely used to purify the plasma membrane of spinach leaf cells in view of its biochemical, structural, and functional characterization in the course of growth and flowering (Penel et al. 1988, Crespi et al. 1989, Greppin et al. 1991). Part of our structural information was acquired by classical EM, with observations of ultrathin sections performed either in plasma membrane preparations or in leaves. Our objective in this paper is to exploit the tremendous potentialities of the AFM to go further in our knowledge of this membrane namely its topographical organization, under physiological conditions, without particular preparation so crucial in EM. We focus our attention on the determination of the conditions for exploring in buffer the surface of purified plasma membrane. Our results demonstrate that features were observed on the plasma membrane surface that were comparable to those described by AFM on the surface of plasma membranes from other biological samples.

Material and methods

Plant material

Spinach plants (*Spinacia oleracea* L. cv. Nobel; Samen Mauser, Winterthur, Switzerland) were grown four weeks in a growth chamber with short-day illumination (8 h daily). The temperature was set at 23 ± 0.5 °C and the relative humidity was maintained at 80% ± 10% during the day and 60% ± 10% during the night. Light (400 μmol/m^2 · s) was provided by white fluorescent tubes (22432-O; Sylvania, Danvers, Mass., U.S.A.).

Plasma membrane isolation

Isolation of pure plasma membrane from spinach leaves was performed by phase partitioning in an aqueous polymer two-phase system (Kjellbom and Larsson 1984), from a crude extract prepared as follows. Leaves (20 g) were homogenized in 80 ml of medium containing 50 mM HEPES (pH 7.5), 500 mM sucrose, 10 mM KCl, 1 mM $MgCl_2$, and 10 mM ascorbic acid. After a centrifugation at low speed (6,000 **g**, 10 min), membranes were collected by high-speed centrifugation (30,000 **g**, 30 min). The crude membrane pellet was used for phase partitioning and the upper fraction obtained at the end of the partition was centrifuged at 30,000 **g** for 30 min. The pellet was suspended in 5 mM phosphate buffer (pH 7.5) to which vitamin C (10 mM) was added. The purity of the fraction was routinely checked by EM analyses, on the basis of a morphological and a cytochemical marker to verify its enrichment in plasma membrane vesicles. Membrane thickness was determined on film negatives of vesicles photographed at ×25,000, with the soft Imagenia of a Biocom image analyzer system (Les Ulis, France). Plasma membranes were also identified on the basis of phosphotungstic acid (PTA) staining of sections at low pH as previously reported (Perroud et al. 1997).

AFM imaging

Protein content of the plasma membrane fraction was appreciated by the Bio-Rad micro-assay (Bio-Rad Laboratories, Munich, Federal Republic of Germany) based on the Bradford method (Bradford 1976). Aliquots of 25 μl corresponding to various protein concentrations were applied for 10 min to the surface of freshly cleaved muscovite green mica (New York Mica Co., New York, N.Y., U.S.A.). The samples were then washed three times with buffer to remove membranes that were not firmly attached to the substrate and they were imaged with a Nanoscope III AFM (Digital Instruments Inc., Santa Barbara, Calif., U.S.A.) equipped with a D type scanner (12 μm). Few preparations were observed in air, most of them being imaged in buffer solution. Various V-shaped silicon nitride cantilevers (Park Scientific Instruments, Sunnyvale, Calif., U.S.A.) with spring constant k equal to 0.01 to 0.06 N/m, are mounted on a bimorph which could be modulated normally to the sample surface. The cantilever spring constant k and its resonant frequency v are related by $k = 2 \cdot (\pi v L)^3 W(\rho^3/E)^{1/2}$, where L and W are

the length and the width of the cantilevers, E is the elastic modulus in the vertical direction, and ρ the density of the material of the cantilever. In order to remove the contaminants, the tips were exposed to UV ozone for 10 min. The UV-ozone cleaning permits the removal of the hydrocarbons. In contact mode the force was previously adjusted for each scan image at the lowest possible value (i.e., about 20 pN). The measured forces after imaging never exceeded 100 pN. In oscillating-contact mode (i.e., tapping-mode AFM, TMAFM), the resonance frequency for cantilevers of 10 mN/m spring constant was locked at 29 kHz. According to the experiment, the driven amplitude varied between 1 and 5 nm and corresponded to an energy of 5 to 125 pJ. Such low amplitude corresponds to the amplitude used in MAC mode AFM which senses piconewton forces (Molecular Imaging, Phoenix, Ariz., U.S.A.). The setpoint was adjusted such that the damping represented less than 20% of the driven amplitude. All reported images were made with 512 by 512 pixels definition with typical scan rates of 1–5 Hz. No striking difference between height images in contact and oscillating-contact modes were recorded. Images of the local viscoelastic properties of the membranes can be obtained in the contact mode from force versus distance curves (Weisenhorm et al. 1993) or by force modulation (Radmacher et al. 1992). In force modulation mode, we have recorded the amplitude and the phase of the oscillation signal corresponding in first approximation to the local elasticity and local viscosity. In this case, the resonance frequency was locked at 8 kHz. The setpoint was adjusted, from force plots, such that the variation in amplitude for imaging represented less than 5 nm. Amplitude and phase images have been obtained simultaneously with the topographical images. These images can provide information on the lateral heterogeneity in membranes by investigating the local viscoelastic properties.

Results

Electron microscopy results (data not shown) indicated that most membranes in our membrane preparations were 8 nm thick with a typical clear dark-light-dark pattern. In addition the bulk of the vesicles were stained with phosphotungstic acid at low pH. The morphological and cytochemical results indicated that our preparation was composed by 90 to 95% of vesicles derived from plasma membrane with minor contaminating membranes, as in previous experiments (Crespi et al. 1989, Perroud et al. 1997).

In our first AFM assay, plasma membrane vesicles at a protein concentration of 25 µg/ml were adsorbed to freshly cleaved mica and observed in buffer. In these conditions it was very difficult to find a region of the mica surface uncovered by sample. In view of this surprising covering of the mica surface, membranes were imaged either in air at the same protein concentration or in buffer at lower protein concentrations ranging from 20 to 5 µg/ml. A typical overview of a plasma membrane (25 µg of protein per ml) imaged in air is shown in Fig. 1 a. Scanning of large zones (10 by 10 µm) revealed a complex organization of the surface of the membrane sample with a first layer of material that practically covered all the mica surface. However, zones were found in which the underlying mica was imaged (Fig. 1 a). The same observation was made for membranes observed in buffer at protein concentrations of 5 to 10 µg/ml (not shown). Estimates of the apparent thickness of the first layer from the analysis of different sections through such regions where the mica was observed gave values of 6.1 ± 0.5 nm for membranes imaged in air (Fig. 1 b) and of 8.2 ± 0.5 nm for membranes imaged in buffer independently of the protein concentration. As in air, the organization of the sample surface was heterogeneous at low resolution when the membrane preparation was imaged at a protein concentration of 25 µg/ml under phosphate buffer. A first layer covering most of the mica surface was observed, on which stand structures highly heterogeneous in shape and size, corresponding likely to membrane sheets and vesicles, with the presence of both flat and smooth areas.

Using smaller scans, the surface of the first layer appeared relatively smooth in some regions and in other regions covered by different structures as shown in Fig. 2. Some areas were covered exclusively by globular-to-elliptical structures which were heterogeneous in size and emerged from the sample surface (Fig. 2 a). The x-y size of these protrusions ranged from 5 nm for the smallest to 70 nm for the largest. Some of the largest protruding particles appeared associated (Fig. 2 b). Aggregates of smaller protrusions were also imaged in some areas as well as a distribution of protruding particles along lines (Fig. 2 c). Some of these arrangements, which were repeatedly observed on different samples and with different AFM tips, looked like hippocampus (Fig. 2 d). It is noteworthy that the direction of these alignments was different from that of the scanning direction and independent of the AFM probe.

In order to prove that the AFM tip does not induce important modification on the observed structures, we have scanned some areas continuously. In this case, the force applied was adjusted before the first recorded image. It was observed that repetitive scanning of the same area of the preparation every 5 min for 30 min did not create new structures and did not cause noticeable distortion or damage to the sample (Fig. 3 a–c). However, "flip-flop" of some proteins could occur under the applied pressure. In order to get some information as to the chemical nature of the protruding particles, membranes at a concentration of 25 µg/ml were incubated, at room temperature, in the presence of the proteolytic enzyme pronase and then adsorbed on mica. Such a treatment however resulted in the

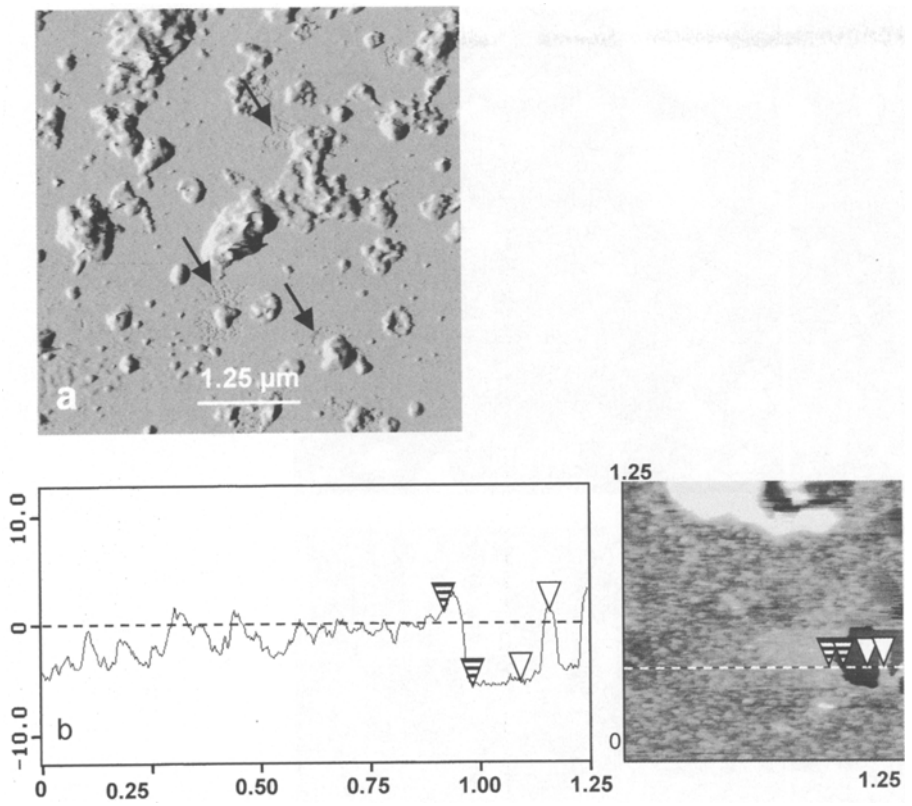

Fig. 1. **a** Imaging in air at low magnification (10 by 10 µm) of plasma membranes from spinach leaves by oscillating-contact mode AFM (TMAFM; deflection mode; scan size, 10 µm; scan rate, 2 Hz; Z range, 0.05 nm). **b** Section analysis showing the thickness of plasma membranes imaged in air. Vertical distances between the pairs of striped and open arrowheads were respectively 6.1 and 6.01 nm

detachment of the sample from the mica surface during scanning. Therefore the enzyme was added in situ to the sample already imaged. Scanning of the same membrane areas before and 30 min after pronase treatment resulted in a net decrease of roughness of the membrane surface in regions covered with particles (Fig. 3d).

In addition to protruding particles as those in Figs. 2 and 3, the presence of channel-like structures was observed in some locations of the samples (Fig. 4). They were frequently found in close proximity to large protruding structures either isolated or aggregated (Fig. 4a). 250 by 250 nm scans indicated that they appeared in most cases composed of 4 subunits disposed around a central hole or depression (Fig. 4b). The diameter of channel structures ranged from 25 to 30 nm (Fig. 4c) and that of their central hole was about 5 nm, estimated from section analysis.

It has to be pointed out that the surface of mica on which buffer alone or PEG in buffer were adsorbed appeared smooth (roughness less than 1 nm) for similar scan sizes as those used for scanning of membranes. Moreover, the different features imaged were repeatedly found upon scanning of plasma membranes purified from different batches of leaves and with two different AFM equipments.

Membrane samples were in some cases kept at 4 °C in buffer to which vitamin C was added, for one or two days before their adsorption on mica. For such samples, the formation of two distinct zones, a smooth and a rough surface on which stand globular structures and channel-like structures, was observed (Fig. 5). For such regions the force modulation mode was used and both phase and topographical signals are given in Fig. 5. The image of the local viscosity (Fig. 5b) shows the phase separation on the membrane, and the topographic image (Fig. 5a) shows the existence of macrodomains in the micrometer range which are embedded in a darker matrix. The step height measured between light domains and the matrix is 0.8 ± 0.1 nm. The same observation was made for plasma membranes scanned next day after their adsorption on mica on which they were kept at room temperature in buffer. AFM images of membranes kept at –80 °C until their examination in buffer were of comparatively lower quality than those of fresh membranes.

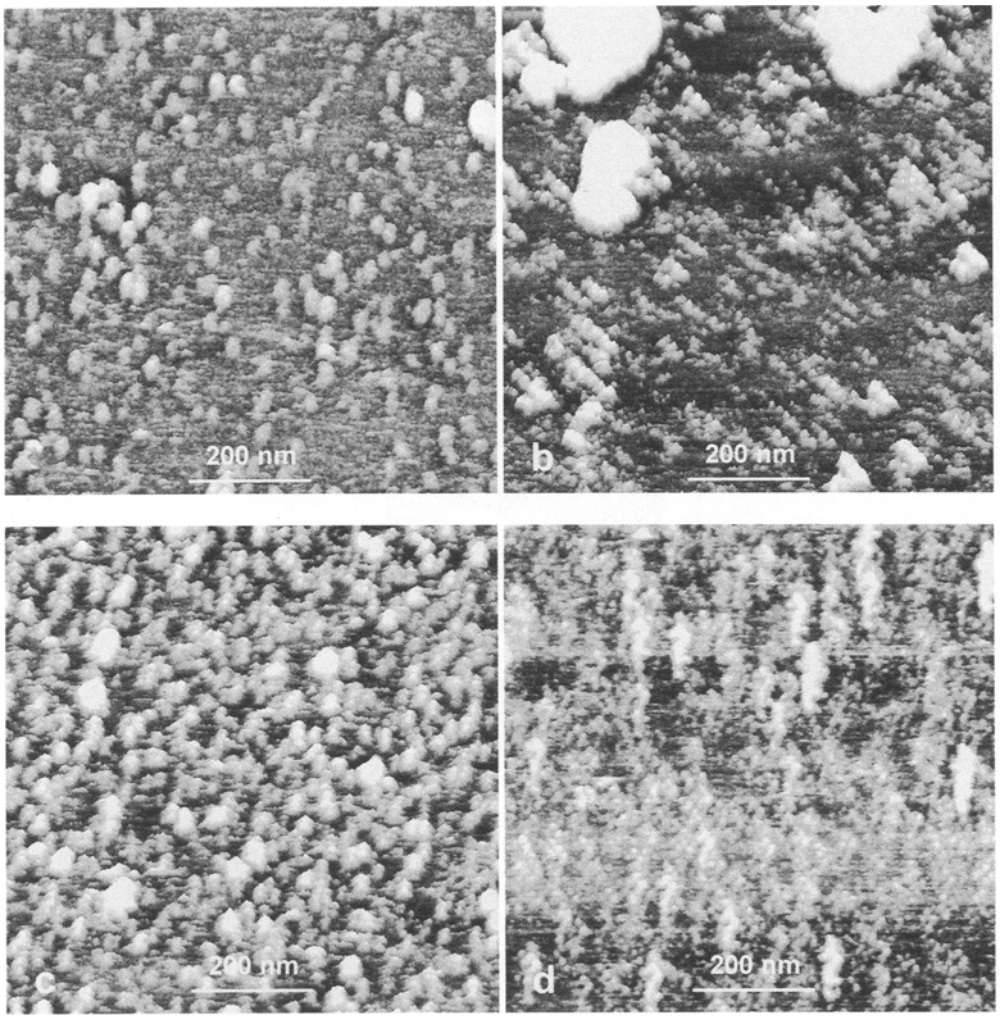

Fig. 2. **a** Submicron scans of the surface of fresh plasma membranes from spinach leaves in phosphate buffer. Globular structures of various sizes were observed. **b–d** AFM images illustrating different arrangements of protruding particles on the plasma membrane surface: alignments and aggregates (**b** and **c**) and hippocampus-like structures (**d**) observed independently of the AFM probe and the scanning direction. (TMAFM; scan size, 800 nm; scan rate, 2 Hz; Z range, 15 nm)

Discussion

Since its appearance in 1986 (Binnig et al. 1986), the AFM has proven to be an excellent tool to investigate structures of many different biological samples (Ratneshwar and Scott 1994, Shao et al. 1996). It has demonstrated its ability to image over a wide range of lateral magnification down to the molecular level, in aqueous environment and without sample preparation technique so crucial in EM. Cell biologists have exploited these remarkable properties of the AFM to study membrane proteins and membrane structure. High-resolution imaging of different membrane proteins such as gap junctions and bacteriorhodopsin has been reported which complements other structural results obtained by negative staining and X-ray crystallography (Butt et al. 1990b; Hoh et al. 1991; Lal et al. 1993; Müller et al. 1995, 1999). Information on the plasma membrane has also been obtained by direct imaging of the surface of intact cells in buffer or in their growth medium, with some features in good agreement again with those obtained by alternative techniques (Lal and John 1994, Lesniewska et al. 1998). So far however there are only a few reports on the use of AFM to study plant cells. Images have been reported for cell wall materials isolated from the parenchyma of different tissues (Kirby et al. 1996) and for pollen grains and cellulose microfibrills (van der Wel et al. 1996). The lower side of leaves from a small Indian tree and from the water lily *Nymphaea odorata*

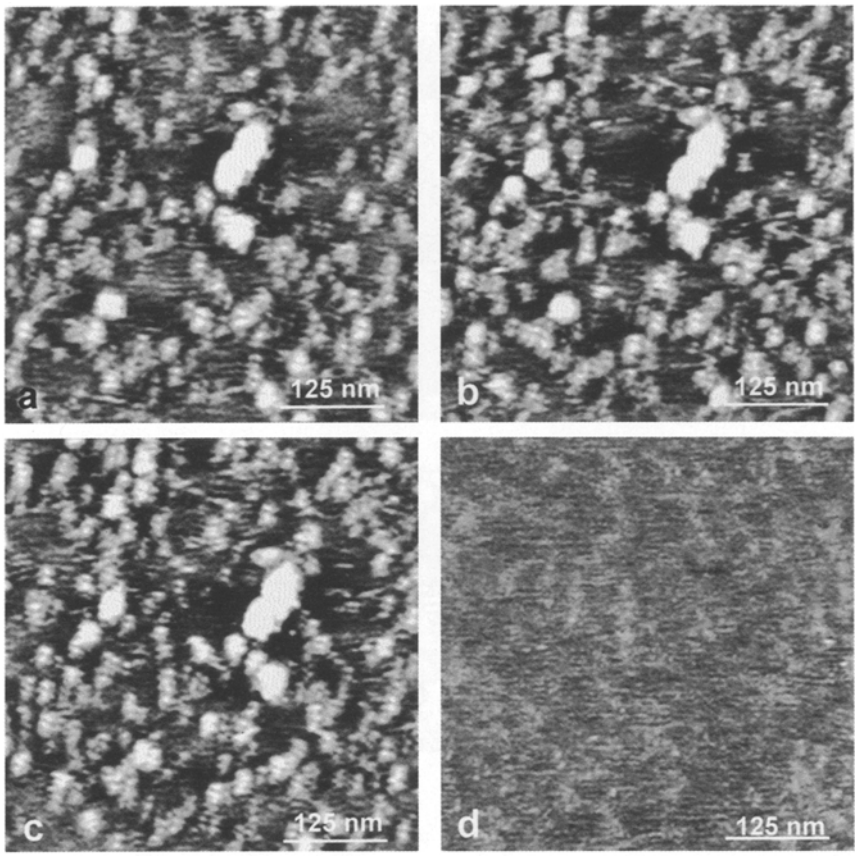

Fig. 3. a–c Three successive images of the same area of the plasma membrane imaged in buffer and recorded after 5, 15, and 30 min. No drastical topographical modification between scans is noticed (TMAFM; scan size, 500 nm; scan rate, 2 Hz; Z range, 20 nm). **d** Image of the same region of the plasma membrane after pronase (0.25% in phosphate buffer) treatment. The mean roughness is decreased by a factor of 2 to 3 (TMAFM; scan size, 500 nm; scan rate, 0.8 Hz; Z range, 20 nm). By using the contact mode AFM we can remove partially the plasma membrane and image the mica surface

has been observed under water but no details below 200 nm were resolved (Butt et al. 1990a).

The AFM images we described here represent the first ones that are concerned with the plasma membrane from plant tissues. This membrane was purified by phase partition, a very current procedure used for its isolation and the fraction obtained was of high purity as checked by EM.

The measured thickness of our membrane on mica is about 6 nm for dry samples and 8 nm for samples examined in buffer. These values were in the same range as those reported for some other biological membranes visualized by AFM and correspond to a single membrane layer. The minimal apparent thickness of plasma membranes from Madin-Darby canine kidney (MDCK) cells grown on glass coverslips gave values close to 6 nm for dried samples and close to 8 nm for living samples in buffer, both values obtained in the flattest zones (Le Grimellec et al. 1995). A similar value of 8 nm was reported for the average thickness of basal cell membranes of MDCK cells prepared by a lysis-squirting protocol and imaged in buffer (Ziegler et al. 1998). The apparent height of the purple membrane examined by AFM in buffer was found to vary from 5.6 nm to 11 nm, depending on the pH of the buffer solution (Butt et al. 1990b, 1991; Müller et al. 1995). The surfaces imaged in the present study most probably correspond to the extracellular surface of the membrane as most vesicles collected from the upper phase of a two-phase system are mainly or exclusively in a cytoplasmic-side-in orientation (Sandelius and Morré 1990). It is likely that upon deposition on mica vesicles opened and maintained this orientation as reported for phospholipid vesicles containing proteins (Contino et al. 1994, Salafsky et al. 1996).

Submicrometer scanning of plasma membrane preparations in buffer revealed the presence of reproducible features, namely protruding particles and channel-like structures. The particles occupy the major part of the surface scanned and are heterogeneous in size. Their minimal size was approximately 15 to 20 nm in air and 4 to 5 nm in buffer, indicating a greater resolution upon imaging in liquid medium.

Protruding particles of different sizes have been described on different membrane surfaces visualized

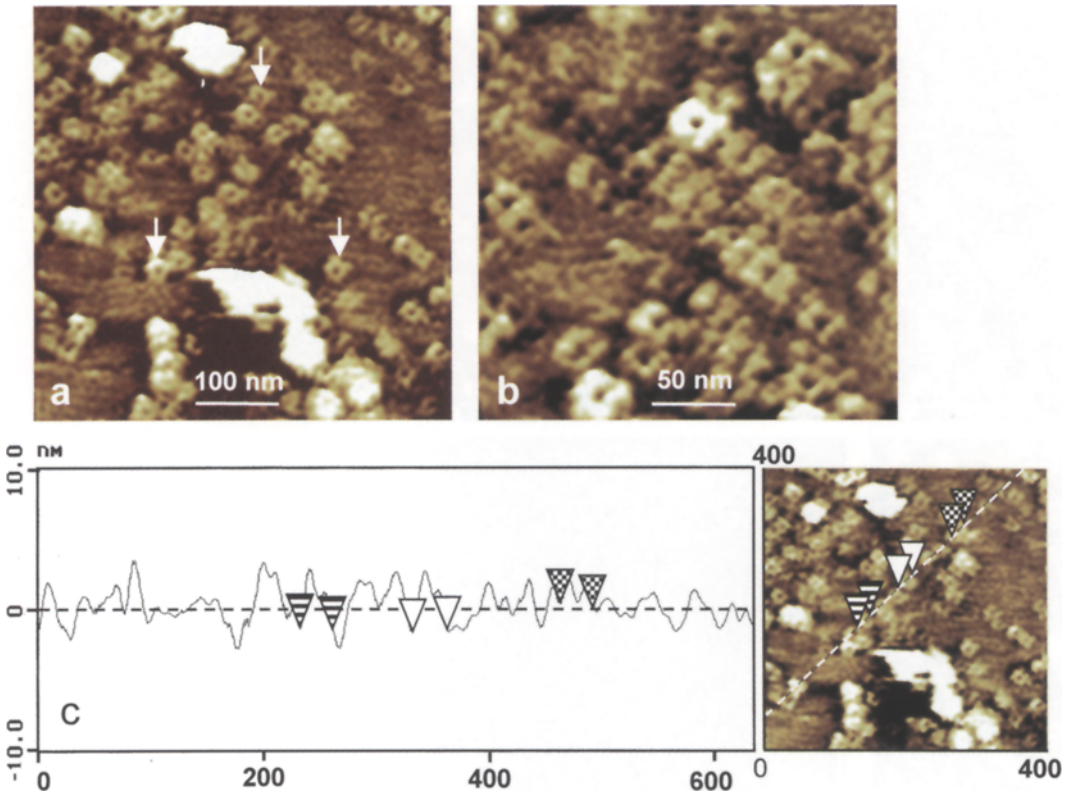

Fig. 4a–c. Imaging at low magnification of plasma membranes from spinach leaves under phosphate buffer. **a** 500 nm scan of the membrane surface to show the presence of channel-like structures (arrows) and a few globular structures (TMAFM; scan size, 500 nm; scan rate, 1 Hz; Z range, 20 nm). **b** 250 nm scan of the membrane surface showing channel-like structures with a central depression (TMAFM; scan size, 250 nm; scan rate, 1 Hz; Z range, 20 nm). **c** Section analysis profile through a channel-like structure. Horizontal distances between the right and middle pairs of arrowheads were respectively 25.5 and 29.4 nm

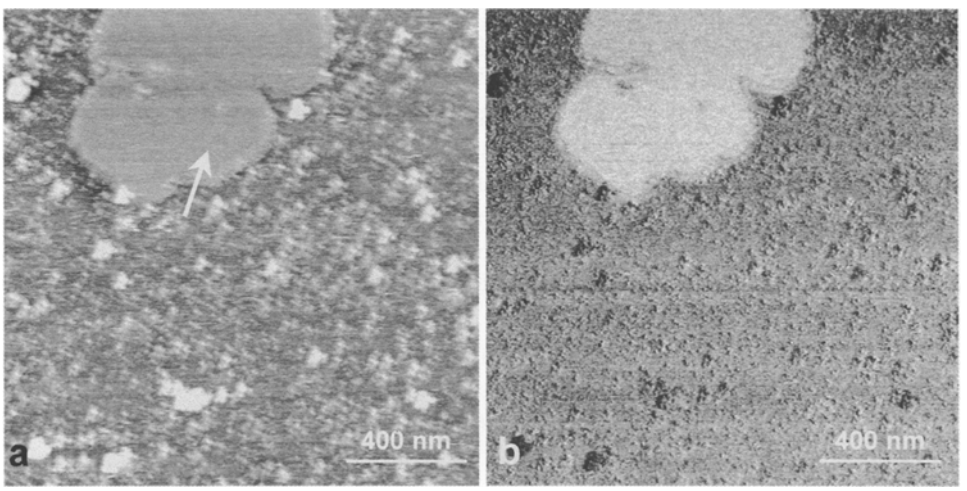

Fig. 5a, b. Imaging at low magnification of plasma membranes from spinach leaves under buffer showing the formation of smooth surfaces (arrow) in the proximity of regions covered with particles (force modulation mode; scan size, 1.6 nm; scan rate, 1 Hz; Z range, 50 nm; phase, 10°). **a** Topography, **b** viscosity

by AFM and were observed on both cytoplasmic (Le Grimellec et al. 1995, Ziegler et al. 1998) and extracellular faces (Le Grimellec et al. 1995, Lärmer et al. 1997) of plasma membrane. Their proteinaceous nature was established by different approaches, namely pronase and gold-labeled-concanavalin A treatments and ethanol dehydration (Häberle et al. 1991, Hörber et al. 1992, Le Grimellec et al. 1994, 1995). The marked decrease of roughness in regions of our samples covered with particles upon the addition of pronase is also in favor of their proteinaceous nature. This protease digests proteins at the membrane surface and reduces the x-y size and the number of protrusions on different plasma membranes visualized by AFM (Le Grimellec et al. 1994, 1995; Lärmer et al. 1997). The fact that particles occupy most of the membrane surface is in agreement with the well-known high protein-to-lipid ratio of this membrane that generally exceeds one (Houslay and Stanley 1982). In spinach a value of 0.98 was reported for plasma membrane (Penel et al. 1988) and a high density of intramembrane particles was observed on freeze-fracture surfaces (Crèvecoeur unpubl.). Such particles were described on most plant plasma membranes visualized by this technique and were generally believed to be integral proteins (Platt-Aloia and Thomson 1989, Webb and Steponkus 1993).

As for other membranes (Hörber et al. 1992; Le Grimellec et al. 1994, 1995; Ziegler et al. 1998), high-magnification AFM reveals that the surface of spinach plasma membrane is heterogeneous with regard to distribution of particles and channels. The heterogeneity was repeatedly found on the major part of the same sample surface and on membranes prepared from different batches of plants. In addition it was observed with both AFM equipments used. It could be attributed to the fact that the plasma membranes came from the different tissues composing spinach leaves, e.g., lower and upper epidermis, palisade and spongy parenchyma, and vascular bundles. They have various roles in the functioning of the leaf. Differences in plasma membrane between different cell types have been revealed by immunocytochemical and biochemical studies. For instance, the auxin transport inhibitor N-1-naphthylphthalamic acid was predominantly localized in pea stems in the plasma membrane of parenchyma cells sheating the vascular bundle (Jacobs and Gilbert 1983). An auxin-binding protein was mainly localized at the plasma membrane of the outer epidermal cells (Löbler and Klämbt 1985). In stems and leaves, plasma membrane H^+-ATPase is essentially present in tissues specialized in nutrient transport like phloem and in guard cells. This localization has been subsequently confirmed by studies of gene expression (DeWitt et al. 1991, Michelet et al. 1994, Michelet and Boutry 1995).

The heterogeneity in membrane surfaces could also be related to distinct microdomains. It has become evident recently that the two membrane faces are organized in plane into a mosaic of supramolecular domains, in plant as well as in animal cells (Edidin et al. 1991, Masson et al. 1992, Edidin 1997).

Distribution of protrusions along lines in a direction different from that of scanning has been reported for AFM imaging of other membrane surfaces (Hörber et al. 1992, Le Grimellec et al. 1995, Ehrenhöfer et al. 1997, Ziegler et al. 1998) and by high-resolution scanning electron microscopy (Walther and Hentschel 1989). In plant cells, arrays of intramembrane particles have been described on plasma membrane surfaces examined by freeze-fracture. They have been related in some cases to ordered membrane-associated synthetic complexes involved in cellulose microfibril biogenesis (Mueller and Brown 1980, Brown et al. 1996, Blanton and Haigler 1996).

In conclusion, our images show that structural information at the nanometer range can be achieved by AFM examination of purified plasma membranes in buffer, without any fixation or preparation. As in other AFM studies of biological membranes, additional experiments are now required to progress in the identification of structures imaged by AFM. However, our first objective in the future will be to compare plasma membranes from vegetative plants and from plants induced to flowering, focusing our interest on mechanical properties of the membrane surface. It was shown that photoperiodic floral induction results in various biochemical and biophysical modifications at the plasma membrane level, some of them indicating a change in membrane fluidity in spinach as well as in other plants (Borochov et al. 1995; Crespi et al. 1993, 1997). We have also the objective to exploit the recognized AFM potential not only as an imaging tool but also as a system for analyzing viscoelastic and mechanical properties of our membrane samples as reported for different living biological cells (Hoh and Schoenenberger 1994, Radmacher et al. 1996) and for artificial membranes (Vié et al. 1998).

Acknowledgments

The authors gratefully acknowledge Mrs. Evelyne Vazquez for her technical participation in preparing plasma membranes. This work was supported by grants from the Région Bourgogne, the Région Languedoc-Roussillon, and the Ministère de la Recherche (France).

References

Binnig G, Quate CF, Gerber CH (1986) Atomic force microscope. Phys Rev Lett 56: 930–933

Blanton RL, Haigler CH (1996) Cellulose biogenesis. In: Smallwood M, Knox P, Bowles D (eds) Membranes: specialized functions in plants. Bios Scientific Publishers, pp 57–75

Borochov A, Spiegelstein H, Halevy AH (1995) Involvement of signal transduction pathway components in photoperiodic flower induction in *Pharbitis nil*. Physiol Plant 95: 393–398

Bradford MM (1976) A rapid and sensitive method for the quantitation of microgram quantities of protein utilizing the principle of protein binding. Anal Biochem 72: 248–254

Brown RM, Saxena IM, Kudlicka K (1996) Cellulose biosynthesis in higher plants. Trends Plant Sci 1: 149–156

Butt HJ, Wolff EK, Gould SAC, Northern BD, Peterson CM, Hansma PK (1990a) Imaging cells with the atomic force microscope. J Struct Biol 105: 54–61

– Downing KH, Hansma PK (1990b) Imaging the membrane protein bacteriorhodopsin with an atomic force microscope. Biophys J 58: 1473–1480

– Prater CB, Hansma PK (1991) Imaging purple membranes dry and in water with the atomic force microscope. J Vac Sci Technol B 9: 1193–1196

Contino PB, Hasselbacher CA, Ross JB, Nemerson Y (1994) Use of an oriented trans-membrane protein to probe the assembly of a supported phospholipid bilayer. Biophys J 67: 1113–1116

Crespi P, Crèvecoeur M, Penel C, Greppin H (1989) Changes in spinach plasmalemma after gibberellic acid treatment. Plant Sci 62: 63–71

– – – (1993) Plasma membrane sterols and flowering induction. Plant Sci 89: 153–160

– Perroud PF, Martinec J, Greppin H (1997) Flowering and membrane functions. In: Greppin H, Penel C, Simon P (eds) Travelling shot on plant development. University of Geneva, Geneva, Switzerland, pp 201–215

Danker T, Mazzanti M, Tonini R, Rakowska A, Oberleithner H (1997) Using atomic force microscopy to investigate patch-clamped nuclear membrane. Cell Biol Int 21: 747–757

DeWitt ND, Harper JF, Sussman MR (1991) Evidence for a plasma membrane proton pump in phloem cells of higher plants. Plant J 1: 121–128

Edidin M (1997) Lipid microdomains in cell surface membranes. Curr Opin Struct Biol 7: 528–532

– Kuo SC, Sheetz MP (1991) Lateral movements of membrane glycoproteins restricted by dynamic cytoplasmic barriers. Science 254: 1379–1382

Ehrenhöfer U, Rakowska A, Schneider SW, Schwab A, Oberleithner H (1997) The atomic force microscope detects ATP-sensitive protein clusters in the plasma membrane of transformed MDCK cells. Cell Biol Int 21: 737–746

Fowke LC (1986) The plasma membrane of higher plant protoplasts. In: Chadwick CM, Garrod DR (eds) Hormones, receptors and cellular interactions in plants. Cambridge University Press, Cambridge, pp 217–239

– (1988) Structure and physiology of the protoplast plasma membrane. Plant Cell Tissue Organ Cult 12: 151–157

– Griffing BG, Mersey BG, Tanchak MA (1986) Protoplasts for studies of cell organelles. In: Fowke CC, Constabel F (eds) Plant protoplasts. CRC Press, Boca Raton, pp 39–52

Greppin H, Bonzon M, Crespi P, Crèvecoeur M, Degli Agosti R, Penel C, Tacchini P (1991) Communication in plants. In: Penel C, Greppin H (eds) Plant signalling, plasma membrane and change of state. Université de Genève, Geneva, Switzerland, pp 139–177

Häberle W, Hörber JKH, Binnig G (1991) Atomic force microscopy on living cells. J Vac Sci Technol B 9: 1210–1213

Henderson E, Haydon PG, Sakaguchi DS (1992) Actin filament dynamics in living glial cells imaged by atomic force microscopy. Science 257: 1944–1946

Heymann JB, Müller DJ, Mitsuoka K, Engel A (1997) Electron and atomic force microscopy of membrane proteins. Curr Opin Struct Biol 7: 543–549

Hoh JH, Schoenenberger CA (1994) Surface morphology and mechanical properties of MDCK monolayers by atomic force microscopy. J Cell Sci 107: 1105–1114

– Lal R, John SA, Revel JP, Arnsdorf MF (1991) Atomic force microscopy and dissection of gap junctions. Science 253: 1405–1408

– Sosinsky GE, Revel JP, Hansma PK (1993) Structure of the extracellular surface of the gap junction by atomic force microscopy. Biophys J 65: 149–163

Hörber JK, Häberle W, Ohnesorge F, Binnig G, Liebich HG, Czerny CP, Mahnel M, Mayr A (1992) Investigation of living cells in the nanometer regime with the scanning force microscope. Scanning Microsc 6: 919–930

Houslay MD, Stanley KK (1982) Dynamics of biological membranes. Wiley, Chichester

Jacobs M, Gilbert SF (1983) Basal localization of the presumptive auxin transport carrier in pea stem cells. Science 220: 1297–1300

Kirby AR, Gunning AP, Waldron KW, Morris VJ, Ng A (1996) Visualization of plant cell walls by atomic force microscopy. Biophys J 70: 1138–1143

Kjellbom P, Larsson C (1984) Preparation and polypeptide composition of chlorophyll-free plasma membranes from leaves of light-grown spinach and barley. Plant Physiol 62: 501–509

Körner LE, Kjellbom P, Larsson C, Møller IM (1985) Surface properties of right-side-out plasma membrane vesicles isolated from barley roots and leaves. Plant Physiol 79: 72–79

Lal R, John SA (1994) Biological applications of atomic force microscopy. Am J Physiol 266: C1–C21

– Kim H, Garavito RM, Arnsdorf MF (1993) Molecular resolution imaging of reconstituted biological channels using atomic force microscopy. Am J Physiol 265: C851–C856

Lärmer J, Schneider SW, Danker T, Schwab A, Oberleithner H (1997) Imaging excised apical plasma membrane patches of MDCK cells in physiological conditions with atomic force microscopy. Pflugers Arch 434: 254–260

Larsson C, Widell S, Kjellbom P (1987) Preparation of high-purity plasma membranes. Methods Enzymol 148: 558–568

Lebrun-Garcia A, Bourque S, Binet MN, Ouaked F, Wendehenne D, Chiltz A, Schaffner A, Pugin A (1999) Involvement of plasma membrane proteins in plant defense responses: analysis of the cryptogein signal transduction in tobacco. Biochimie 81: 663–668

Le Grimellec C, Lesniewska E, Cachia C, Schreiber JP, de Fornel F, Goudonnet JP (1994) Imaging of the membrane surface of MDCK cells by atomic force microscopy. Biophys J 67: 36–41

– – Giocondi MC, Cachia C, Schreiber JP, Goudonnet JP (1995) Imaging of the cytoplasmic leaflet of the plasma membrane by atomic force microscopy. Scanning Microsc 9: 401–411

Leshem Y (1992) Plant membranes biophysics development and senescence. In: Leshem Y (ed) Plant membranes: a biophysical

approach to structure, development and senescence. Kluwer, Dordrecht, pp 113–154

Lesniewska E, Giocondi MC, Vié V, Finot E, Goudonnet JP, Le Grimellec C (1998) Atomic force microscopy of renal cells: limits and prospects. Kidney Int Suppl 65: S42–S48

Löbler M, Klämbt D (1985) Auxin-binding protein from coleoptiles membrane of corn (*Zea mays* L.). J Biol Chem 260: 9854–9859

Masson F, Rakotomavo M, Rossignol M (1992) Characterization in tobacco leaves of structurally and functionally different membrane fractions enriched in vanadate sensitive H^+-ATPase. Plant Sci 92: 129–142

– Santoni V, Rossignol M (1994) Functional and structural changes at the plasma membrane during the induction of flowering in tobacco leaves. Flowering Newsl 17: 39–43

Michelet B, Boutry M (1995). The plasma membrane H^+-ATPase: a highly regulated enzyme with multiple physiological functions. Plant Physiol 108: 1–6

– Lukaszewicz M, Dupriez V, Boutry M (1994) A plant plasma membrane proton-ATPase gene is regulated by development and environment and shows signs of translational regulation. Plant Cell 6: 1375–1389

Mueller SC, Brown RM (1980) Evidence for an intramembrane component associated with a cellulose microfibril synthesizing complex in higher plants. J Cell Biol 84: 315–326

Müller DJ, Schabert FA, Büldt G, Engel A (1995) Imaging purple membranes in aqueous solutions at subnanometer resolution by atomic force microscopy. Biophys J 68: 1681–1686

– Sass HJ, Müller SA, Büldt G, Engel A (1999) Surface structures of native bacteriorhodopsin depend on the molecular packing arrangement in the membrane. J Mol Biol 285: 1903–1909

Oberleithner H, Geibel W, Guggino W, Henderson RM, Hunter M, Schneider SW, Schwab A, Wang W (1997) Life on biomembranes viewed with the atomic force microscope. Wien Klin Wochenschr 109: 419–423

Penel C, Auderset G, Bernardini N, Castillo F, Greppin H, Morré DJ (1988) Compositional changes associated with plasma membrane thickening during floral induction of spinach. Physiol Plant 73: 134–146

Perroud PF, Crespi P, Crèvecoeur M, Fink A, Tacchini P, Greppin H (1997) Detection and characterization of GTP-binding proteins on tonoplast of *Spinacia oleracea*. Plant Sci 122: 23–33

Platt-Aloia KA, Thomson WW (1989) Advantages of the use of intact plant tissues in freeze-fracture electron microscopy. J Electron Microsc 13: 289–299

Quinn PJ, Williams WP (1990) Structure and dynamics of plant membranes. In: Marwood JL, Bowyer JR (eds) Methods in plant biochemistry, vol 4. Academic Press, pp 297–340

Radmacher M, Tillmann RW, Fritz M, Gaub HE (1992) From molecules to cells: imaging soft samples with the atomic force microscope. Science 257: 1900–1905

– Fritz M, Kacher CM, Cleveland JP, Hansma PK (1996) Measuring the viscoelastic properties of human platelets with the atomic force microscope. Biophys J 70: 556–567

Rakowska A, Danker T, Schneider SW, Oberleithner H (1998) ATP-induced shape change of nuclear pores visualized with the atomic force microscope. J Membr Biol 163: 129–136

Ratneshwar L, Scott AJ (1994) Biological applications of atomic force microscopy. Am J Physiol 266: C1–C21

Salafsky J, Groves JT, Boxer SG (1996) Architecture and function of membrane proteins in planar supported bilayers: a study with photosynthetic reaction centers. Biochemistry 35: 14773–14781

Sandelius AS, Morré DJ (1990) Plasma membrane isolation. In: Larsson C, Moller JM (eds) The plant plasma membrane. Springer, Berlin Heidelberg New York Tokyo, pp 44–75

Sandstrom RP, de Boer AH, Lomax TL, Cleland RH (1987) Latency of plasma membrane H^+-ATPase in vesicles isolated by aqueous phase partitioning. Plant Physiol 85: 693–698

Schabert F, Henn C, Engel A (1995) Native *Escherichia coli* OmpF porin surfaces probed by atomic force microscopy. Science 268: 92–94

Shao Z, Mou J, Czajkowski DM, Yang J, Yuan JY (1996) Biological atomic force microscopy: what is achieved and what is needed. Adv Phys 45: 1–86

van der Wel NN, Putman CAJ, van Noort SJT, de Grooth BG, Emons AMC (1996) Atomic force microscopy of pollen grains, cellulose microfibrils and protoplasts. Protoplasma 194: 29–39

Vié V, Van Mau N, Lesniewska E, Goudonnet JP, Heitz H, Le Grimellec C (1998) Distribution of ganglioside GM_1 between two-component, two-phase phosphatidylcholine monolayers. Langmuir 14: 4574–4583

Walther P, Hentschel J (1989) Improved representation of cell surface structure by freeze substitution and backscattered electron imaging. Scanning Microsc Suppl 105: 201–211

Webb MS, Steponkus PL (1993) Freeze-induced membrane ultrastructural alterations in rye (*Secale cereale*) leaves. Plant Physiol 101: 955–963

Weisenhorm AL, Khorsandi M, Kasas S, Gotzos V, Butt HJ (1993) Deformation and height anomaly of soft surfaces studied with an AFM. Nanotechnology 4: 106–113

Ziegler U, Vinckier A, Kernen P, Zeisel D, Biber J, Semenza G, Murer H, Groscurth P (1998) Preparation of basal cell membranes for scanning probe microscopy. FEBS Lett 436: 179–174